IL NUOVO CIMENTO Vol. 34 C, N. 4 Luglio-Agosto 2011
DOI 10.1393/ncc/i2011-10982-x

Colloquia: Channeling 2010

Long-distance transfer of microwaves in sliding-mode virtual plasma waveguides

V. D. Zvorykin, A. O. Levchenko, I. V. Smetanin and N. N. Ustinovskii
P.N. Lebedev Physical Institute - Leninskii Pr. 53, 119991 Moscow, Russia

(ricevuto il 22 Dicembre 2010; pubblicato online il 22 Settembre 2011)

Summary. — Experimentally an effective channeling and transfer of the sliding mode of the 35.3 GHz ($\lambda \approx 8.5$ mm) microwave signal along 60 m distance has been demonstrated in the low-density ($n_e \sim 10^{12}\,\mathrm{cm}^{-3}$) 10 cm diameter hollow plasma waveguide created by the 100 ns UV pulse of GARPUN KrF laser in the laboratory air. The mechanism of the transfer is the total internal reflection of the signal on the optically less dense walls of the waveguide. The theory of this sliding mode propagation in large-diameter ($D \gg \lambda$) plasma waveguides is developed, which is in good accordance with our experimental results.

PACS 52.40.Db – Electromagnetic (nonlaser) radiation interactions with plasma.
PACS 07.57.-c – Infrared, submillimeter wave, microwave and radiowave instruments and equipment.

1. – Introduction

The recent revival of interest in the transfer of high-power electromagnetic (microwave and radiofrequency) radiation pulses in atmospheric air using a laser plasma as a guiding structure has been stimulated by the discovery of filamentation of high-power ultrashort laser pulses in atmospheric-pressure gases [1-3]. In the process of filamentation, when a laser pulse propagates in atmospheric-pressure gases, a trace is formed in the shape of a thin plasma filament $\leq 100\,\mu$m in diameter, electron density 10^{15}–$10^{17}\,\mathrm{cm}^{-3}$, and several hundred meters long. The propagation of microwave radiation in hollow plasma waveguides, whose walls are formed by these filaments, was theoretically investigated in [4]. The optimum choice of the plasma waveguide radius was found to be of the order of the wavelength of the signal, $R \sim \lambda$. In this case, the transfer regime is provided by the high conductance of the plasma in the channel; thus, the physical mechanism is quite similar to the traditional case of waveguides with metal walls. The conductivity of plasma, however, is several orders of magnitude lower than that of metal and, as a result, the signal propagates only to a small distance. In the experiment [5], the 10 GHz microwave signal was transferred to a distance of only $\sim$ 16 cm in the waveguide of ~ 4.5 cm in diameter formed by multiple filaments.

In this work, we investigate experimentally and theoretically an alternative mechanism of the sliding-mode propagation of microwave radiation inside a hollow plasma channel of large radius $R \gg \lambda$ [6, 7], which makes it possible to increase significantly the signal transfer length. Such a possibility with the use of a tubular UV laser beam was first indicated in [8]. Physically, this mechanism is based on the effect of total reflection at the interface with an optically less dense medium. For waveguides of a sufficiently large radius, lower modes become "sliding"—the transverse wave number is significantly ($\sim \lambda/R$ times) smaller than the longitudinal wave number, and the effective angle of incidence on the reflection surface exceeds the critical angle determined by the ratio of the refraction indices of air and plasma. With this approach, high conductivity of the plasma is not required, which makes it possible to use low ionization degrees of air, with plasma density of 10^{11}–$10^{14}\,\mathrm{cm}^{-3}$ [6, 7].

We should emphasize the difference between plasma waveguides used in our work and large-radius dielectric waveguides [9, 10]. Those waveguides are, in particular, capillary tubes with dielectric walls; high-power laser radiation propagating in the waveguides ionizes the gas filling the capillary tube and generates the plasma wave for acceleration of electrons [11-13]. The mode analysis of such a structure is presented in [10]. In such dielectric waveguides, reflection occurs at the boundary of the wall with larger permittivity than inside the capillary, and the losses emerge owing to the leakage of radiation through the capillary wall. In contrast, in plasma waveguides, there exists total internal reflection from the optically less dense walls, and the modes are attenuated owing to the plasma conductivity.

2. – Experimental realization of sliding modes in plasma waveguides

Below, we present the results of the first experiments on the efficient channeling and transfer of the sliding mode of a microwave signal in a plasma waveguide of a comparatively large radius $R \approx 5\,\mathrm{cm}$ formed in atmospheric air by the radiation of a GARPUN KrF excimer laser [14]. In the unstable-resonator injection control regime, the laser generated pulses of $\sim 70\,\mathrm{ns}$ FWHM, an energy of $\sim 50\,\mathrm{J}$, and radiation divergence $\sim 10^{-4}\,\mathrm{rad}$. To obtain a parallel, convergent or divergent "tubular" beam, we used various optical arrangements (see fig. 1).

In the scheme (a), the central part 100–120 mm in diameter was shut in the initial laser beam $180 \times 160\,\mathrm{mm}$ in transverse size by means of a round closure. Herewith, the average radiation intensity (in the beam cross-section) did not exceed $I = 2 \cdot 10^6\,\mathrm{W/cm}^2$, and the photoelectron density in air was, according to the plasma conductivity measurements [15], $n_e \sim 2 \cdot 10^8\,\mathrm{cm}^{-3}$. To increase the electron density by three orders of magnitude, readily ionized hydrocarbon vapors were added to atmospheric air.

In the scheme (b), the initial beam was compressed by a two-lens telescope and, with the use of two axicons (conical lenses), was transformed without energy losses into a tubular beam 120 mm in outer diameter and 10 mm "wall" thickness. In this scheme, the average radiation intensity in the ring was $I = 10^7\,\mathrm{W/cm}^2$, the electron density increased in air up to $n_e \sim 10^9\,\mathrm{cm}^{-3}$ and, correspondingly, upon the addition of hydrocarbons, up to $n_e \sim 10^{12}\,\mathrm{cm}^{-3}$. The tubular beam in these experiments was convergent: its diameter decreased by a factor two at a distance of about 15 m along the axis.

In the variant (c) of the arrangement, we used single axicon, and the tubular beam diverged with the cone angle of 2.4°. And in the variant (d), a combination of an axicon and a lens was used, which decreased the cone angle of the divergent tubular beam down to $\sim 1°$.

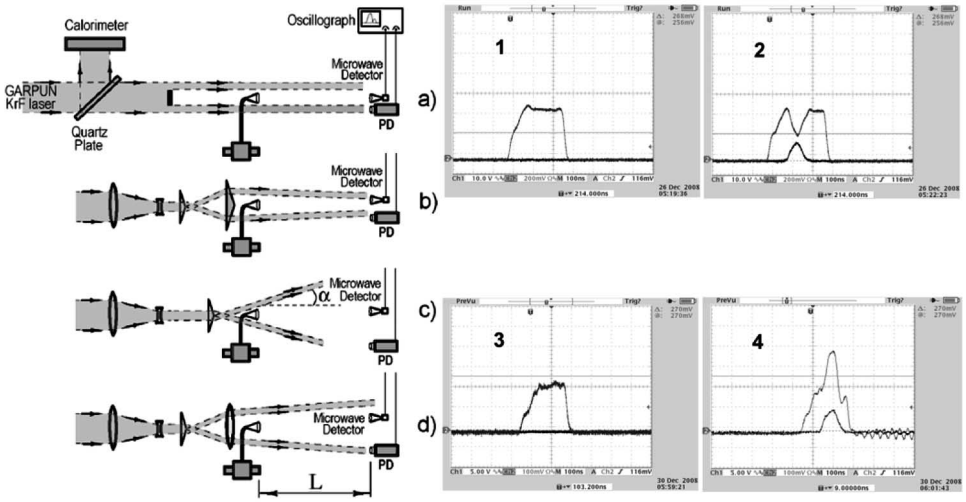

Fig. 1. – Layout of experiments on the microwaves propagation in plasma waveguides (left); oscillograms of microwave pulse without (1, 3) and with laser pulse (2, 4) (right). Lower traces represent laser pulses and upper traces microwave signals. Oscillograms 1 and 2 correspond to scheme (a), 3 and 4 to scheme (d).

As a source of microwave radiation, we used a pulsed magnetron with a peak output power of 20 kW at a frequency of 35.3 GHz ($\lambda \approx 8.5$ mm). The microwave source was equipped with a 30°-conical horn transmitter antenna 25 mm in outer diameter, the microwave radiation receiver with the same horn was positioned at various distances L from the emitter. In pure air, no noticeable change of the microwave signal was observed in the presence of a tubular laser beam in either of the schemes studied. The reason for this was the insufficient photoelectron density responsible for the formation of a virtual plasma waveguide. Upon addition of hydrocarbon vapors along the propagation route, we observed the interaction of the microwave radiation with the photoionized plasma of the waveguide. Characteristic signals from the receiver and a synchronized laser pulse are shown in the right-hand side of fig. 1.

Depending on the scheme of the experiments and the laser radiation intensity (respectively, the electron density in the waveguide wall), we observed that during the laser pulse the microwave signal either was absorbed in the scheme (a) (see oscillogram 2 in fig. 1) or increased in the schemes (c) and (d) (oscillogram 4 in fig. 1). The largest increase in the microwave-signal amplitude, up to 6 times, was observed in the scheme (d) at a distance $L = 60$ m from the emitter to the receiver. In the scheme (b), where the tubular laser beam converged, the microwave signal almost did not change.

The mechanism of microwave radiation channeling in a weakly ionized plasma waveguide is related to the reflection of radiation from the electron-density gradient at the plasma-air interface. This effect is similar to total internal reflection of optical radiation in optical fibers, but differs by the occurrence of microwave radiation in the waveguide plasma. The sign of the effect (amplification or absorption of microwave radiation) is determined by the balance of these two factors. Thus, absorption predominates at low laser intensities and electron densities in the scheme (a) of our arrangement. At higher laser intensities in the schemes (c) and (d), the microwave radiation is amplified due to

its channeling.

A qualitative condition for the microwave-radiation channeling in a geometric approximation (strictly speaking, true when the waveguide diameter $D \gg \lambda$) is that the characteristic diffraction angle of the transported microwave mode $\vartheta \sim \lambda/D$ is smaller than the angle of total internal reflection Θ determined by the relation $\cos\Theta = n$, where n is the refraction index of ionized gas with respect to air. For small sliding angles, the expression for Θ is transformed to the form $\Theta^2 \approx \Omega_p^2/(\omega^2+\nu_T^2)$, where $\Omega_p = \sqrt{4\pi n_e e^2/m_e}$ is the plasma frequency and ν_T is the characteristic transfer frequency of electron collisions.

The interaction length of microwave radiation and plasma in a weakly converging waveguide (scheme (d) in fig. 1) was assessed experimentally by closing the laser beam with a dielectric screen at various distances from the microwave source; the interaction length was found to be about 10 m.

3. – Theory of the sliding-mode propagation in plasma waveguides

To develop a theory of the sliding mode propagation which has been realized in our experiment, we make use of a simplified model. We consider the electromagnetic modes of a circular waveguide of constant radius $R \gg \lambda$ which is the air cylinder bounded by a plasma layer. Thickness of the plasma walls is assumed to be much larger than the field-penetration depth. Characteristic depletion distance of the UV excimer laser radiation in air is well above the waveguide length, and one can consider the plasma waveguide to be homogeneous and of a constant density. The diffuse spreading of the waveguide walls is assumed to be small compared to the microwave-signal wavelength λ.

At our experimental conditions, dielectric properties of the weakly-ionized ($n_e \leq 10^{15}$–$10^{16}\,\mathrm{cm}^{-3}$) air plasma are determined by the effective momentum transfer rate of collisions of electrons with air molecules, which can be estimated at atmospheric pressure and characteristic electron temperature of 0.03–1 eV as $\nu_T \sim 10^{12}\,\mathrm{s}^{-1}$ [16-18]. The permittivity of atmospheric air for the centimeter-submillimeter wavelengths is $\varepsilon_{\mathrm{air}} - 1 \sim 10^{-4}$ [16], so this difference can be neglected, assuming $\varepsilon_{\mathrm{air}} = 1$. Thus, within the centimeter-submillimeter wavelength range, the following relation of the real and imaginary parts is fulfilled:

$$\mathrm{Re}(1-\varepsilon_p) = \frac{\xi}{1+\omega^2/\nu_T^2} \ll \mathrm{Im}(1-\varepsilon_p) = \frac{\xi}{1+\omega^2/\nu_T^2}\frac{\nu_T}{\omega}\,. \tag{1}$$

Here, $\xi = \Omega_p^2/\nu_T^2 \approx 3.19\cdot 10^{-3}\cdot(n_e/10^{12}\,\mathrm{cm}^{-3})$ at the plasma density $n_e \leq 10^{15}\,\mathrm{cm}^{-3}$. This particular feature, as we discussed above, distinguishes plasma waveguides from dielectric waveguides [9, 10].

In the considered waveguides with $R \gg \lambda$, the conditions of internal reflection are, obviously, fulfilled more easily at a smaller characteristic angle of the sliding mode (*i.e.* the closer the angle of "incidence" on the waveguide wall to $\pi/2$); due to this fact, we choose as operating modes the lowest axial-symmetric transverse magnetic (TM) E_{01} and transverse electric (TE) H_{01} modes, as well as the EH_{11} mode, which is known to be the main operating mode in dielectric waveguides [9].

For the axial-symmetric modes, the electromagnetic field components are E_z, E_r, H_ϕ for the TM mode E_{0n} and H_z, H_r, E_ϕ for the TE mode H_{0n}. The longitudinal components of these modes are described by $\sim J_0(\kappa_1 r)\exp[i(hz-\omega t)]$ inside the waveguide and $\sim H_0^{(1)}(\kappa_2 r)\exp[i(hz-\omega t)]$ in the plasma of the walls, r and z are the transverse

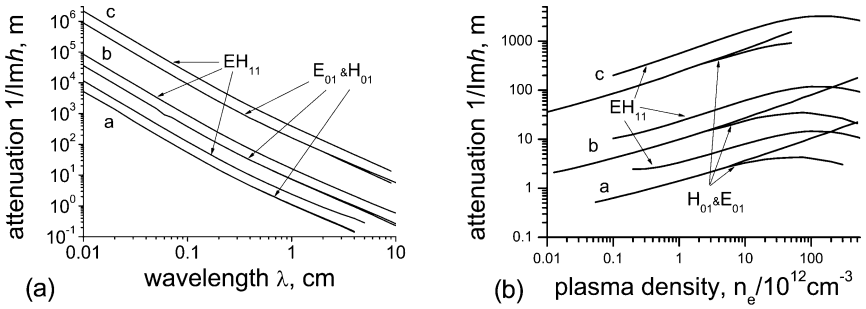

Fig. 2. – The characteristic propagation distance $(\mathrm{Im}\, h)^{-1}$ of the sliding axial-symmetric modes (E_{01} and H_{01}) and the hybrid mode EH_{11} (a) as a function of wavelength at the fixed plasma density $n_e = 10^{12}\,\mathrm{cm}^{-3}$ and (b), as a function of density at given wavelength $\lambda = 8\,\mathrm{mm}$. The calculations are made for the plasma waveguide radii $R =$ curve a 5 cm, curve b 10 cm, and curve c 30 cm.

and longitudinal coordinates (the cylindrical coordinate system is used). Here and below, the functions $J_n(x)$ and $H_n^{(1)}(x)$ are Bessel functions and Hankel functions of the first kind, the transverse wave numbers are determined by the dispersion relations in air, $\kappa_1^2 = k_0^2 - h^2$ and plasma, $\kappa_2^2 = \varepsilon_p k_0^2 - h^2$, respectively, $k_0 = \omega/c$ is the wave number in vacuum. The boundary conditions determine the dispersion equation [19]

$$\frac{1}{\kappa_1 R}\frac{J_1(\kappa_1 R)}{J_0(\kappa_1 R)} = \frac{\chi}{\kappa_2 R}\frac{H_1^{(1)}(\kappa_2 R)}{H_0^{(1)}(\kappa_2 R)}\,, \tag{2}$$

where $\chi = \varepsilon_p$ stands for the TM axial-symmetric modes, and $\chi = 1$ for the TE modes.

The lowest axial-asymmetric mode EH_{11} is a hybrid mode, *i.e.* it contains all six components of the electromagnetic field; herewith, all longitudinal components of the electric and magnetic fields have the form $E_z, H_z \sim J_1(\kappa_1 r)$ inside the waveguide and $E_z, H_z \sim H_1^{(1)}(\kappa_2 r)$ in plasma of the walls. The dispersion equation for the mode EH_{11} is [19]

$$\begin{aligned}&\left[\left(\frac{1}{\kappa_1}\frac{J_0(\kappa_1 R)}{J_1(\kappa_1 R)} - \frac{\varepsilon_p}{\kappa_2}\frac{H_0^{(1)}(\kappa_2 R)}{J_1(\kappa_2 R)}\right) - \left(\frac{1}{\kappa_1^2 R} - \frac{\varepsilon_p}{\kappa_2^2 R}\right)\right] \\ &\times\left[\left(\frac{1}{\kappa_1}\frac{J_0(\kappa_1 R)}{J_1(\kappa_1 R)} - \frac{1}{\kappa_2}\frac{H_0^{(1)}(\kappa_2 R)}{J_1(\kappa_2 R)}\right) - \left(\frac{1}{\kappa_1^2 R} - \frac{1}{\kappa_2^2 R}\right)\right] = \left(\frac{1}{\kappa_1^2 R} - \frac{\varepsilon_p}{\kappa_2^2 R}\right)\left(\frac{1}{\kappa_1^2 R} - \frac{1}{\kappa_2^2 R}\right).\end{aligned} \tag{3}$$

Since $R/\lambda \gg 1$, dispersion equations (2), (3) have, generally speaking, a number of roots corresponding to various transverse axial-symmetric modes. The greatest propagation length corresponds, apparently, to the minimum value of the transverse wave number κ_1, *i.e.* to the lowest transverse mode.

The dispersion equations (2), (3) can be easily solved numerically. Figure 2 presents the characteristic propagation distance $(\mathrm{Im}\, h)^{-1}$ of the sliding axial-symmetric modes (E_{01} and H_{01}) and the hybrid mode EH_{11} of a plasma waveguide (a) *versus* the signal wavelength within the centimeter-submillimeter wave range at the plasma density $n_e = 10^{12}\,\mathrm{cm}^{-3}$, and (b) *versus* the plasma density at the wavelength $\lambda = 8.5\,\mathrm{mm}$. The

calculations were carried out for various values of the waveguide radius $R = 5$, 10, 30 cm; the characteristic transfer frequency was taken to be $\nu_T = 10^{12}\,\mathrm{s}^{-1}$.

As one can find from fig. 2a, the characteristic propagation distance $(\mathrm{Im}\,h)^{-1}$ is larger for the hybrid mode EH_{11}, and the results for the E_{01} and H_{01} modes practically coincide; some discrepancy begins only at wavelengths $\lambda \geq 1$ cm. With the increase in plasma density, the propagation distance $(\mathrm{Im}\,h)^{-1}$ for the modes E_{01} and EH_{11} starts to decrease, whereas it increases for the magnetic mode H_{01}.

To analyze the roots of the dispersion equations (2), (3), it is convenient to introduce the dimensionless parameter $\mu^2 = (k_0 R\Omega_p/\nu_T)^2/(1 + (\omega/\nu_T)^2)$. Setting $\kappa_1 R = x\mu$ and $\kappa_2 R = y\mu$, we have $x^2 - y^2 = 1 - i\nu_T/\omega$, and the solutions of dispersion equations are, in fact, determined by two parameters, μ and ν_T/ω. Numerical analysis makes it possible to determine the threshold value of the parameter μ at which the effective propagation of the sliding mode is possible,

$$\mu_{\mathrm{th}} \approx 1. \tag{4}$$

In the range of parameters $\mu \sim 0.5$–1, absorption sharply increases, and at $\mu \leq 0.5$ the propagation almost vanishes—the characteristic propagation length $(\mathrm{Im}\,h)^{-1}$ is limited to several wavelengths. In the domain $\mu > \mu_{\mathrm{th}} = 1$, the propagation regime is stabilized. As $\mu^2 \propto n_e R^2$, relation (4), in fact, determines the lower boundary of plasma densities and waveguide radii at which the sliding propagation regime is realized.

In the limit of large values

$$\mu \gg 1, \qquad \nu_T/\omega \gg 1, \tag{5}$$

we succeed in obtaining simple analytical relations, by analogy with those done for large-radius dielectric waveguides [10]. It is easy to see that the root of the dispersion equation (2) occurring near the point $x \approx \alpha/\mu$, where $\alpha \approx 3.83$ is the first root of the Bessel function $J_1(\alpha) = 0$, corresponds to the sliding regime for the lowest axial-symmetric modes E_{01} and H_{01}. The lowest root of dispersion equation (3) is near $\mu x \approx \beta \approx 2.405$ $(J_0(\beta) = 0)$. For this, it is necessary that

$$|\varepsilon_p| \ll k_0 R\sqrt{\xi\nu_T/\omega}, \tag{6}$$

In this case, one can find $y^2 = i\nu_T/\omega + x^2 - 1$ whence, for the characteristic transverse wave number in the plasma of the waveguide wall, we obtain

$$\kappa_2 = \frac{\mu y}{R} \approx \pm(1+i)\frac{\mu}{R}\sqrt{\frac{\nu_T}{2\omega}}\,, \tag{7}$$

where the plus sign should be chosen to provide the decay of the field in the plasma with the radius $r > R$.

Thus, as we demonstrated numerically above (see fig. 2), for plasma with a low degree of ionization, such that $|\varepsilon_p - 1| \ll 1$ (*i.e.* $\xi\nu_T/\omega \ll 1$), the solutions for the E_{01} and H_{01} modes practically coincide, and for the attenuation coefficient we have

$$\mathrm{Im}\,h \approx \frac{\alpha^2}{k_0^2 R^3\sqrt{2\xi\nu_T/\omega}}\,. \tag{8}$$

For the decrement of the hybrid EH_{11} mode, we obtain

$$\operatorname{Im} h \approx \frac{\beta^2}{k_0^2 R^3 \sqrt{2\xi\nu_T/\omega}}, \tag{9}$$

The characteristic propagation length of the hybrid mode EH_{11} exceeds the propagation length of the axial-symmetric modes $(\alpha/\beta)^2 \approx 2.54$ times. It scales with the frequency of the signal and plasma waveguide radius as $(\operatorname{Im} h)^{-1} \propto R^3\omega^{3/2}n_1^{1/2}$, and this behavior is supported by our numerical investigation given in fig. 2.

With increase in the plasma density in the domain $k_0R \gg \sqrt{\xi\nu_T/\omega} \gg 1$ (in this case, condition (6) is still valid), the solutions for axially-symmetric modes split as shown in fig. 2b. For the mode H_{01}, the root of the dispersion equation remains near $x \sim \alpha/\mu$, and relation (8) is preserved. For the mode E_{01}, the root is gradually shifted with increase in density, $(\mu x - \alpha)/\alpha \propto \sqrt{\xi\nu_T/\omega}/k_0R$, and for the decrement of attenuation of this mode we derive

$$\operatorname{Im} h \approx \frac{\alpha^2}{k_0^2 R^3}\sqrt{\frac{\xi\nu_T}{2\omega}}\left(1 + \frac{1}{k_0 R}\sqrt{\frac{\xi\nu_T}{2\omega}}\right), \tag{10}$$

and for the hybrid mode EH_{11}

$$\operatorname{Im} h \approx \frac{\beta^2}{k_0^2 R^3}\sqrt{\frac{\xi\nu_T}{2\omega}}, \tag{11}$$

i.e. its characteristic propagation length begins to decrease with density, $\propto n_e^{-1/2}$ (see fig. 2b).

Transition to the regime of a metal waveguide occurs with further density increase and shifts to the domain $\sqrt{\xi\nu_T/\omega} \gg k_0R$, when relation (6) ceases to be fulfilled. In this regime of high conductance of the walls, the coefficient on the right-hand side of (2) becomes large, $|\xi/\kappa_2 R| \gg 1$, and, as a consequence, the root of the dispersion equation for the E_{01} mode shifts to the value $\mu x \approx \beta \approx 2.405$ ($J_0(\beta) = 0$), which is characteristic of the E_{01} mode of a metal waveguide. In accordance with the theory of metal waveguides, the attenuation decrement of such a TM mode increases with frequency, $\operatorname{Im} h \propto \sqrt{\omega}$, and its minimum value is achieved near the cutoff frequency [9]. In this range of parameters, the optimum propagation conditions are realized at $R \sim \lambda$ [4, 5].

4. – Conclusions

To conclude, in this paper we presented the results of a theoretical and experimental study of the sliding mode of the microwave radiation transfer in plasma waveguides in atmospheric air. The mechanism of the transfer is based on the effect of total reflection at the interface with an optically less dense medium and does not require high conductance (density) of plasma. The transfer of a microwave signal, $\lambda = 8.5$ mm, to a distance over 60 m was experimentally demonstrated. The results of calculations are in good agreement with the experiment and convincingly demonstrate the advantage of the sliding-mode propagation in comparison with high-density plasma waveguides—the power inputs for a waveguide to be developed prove to be lower, and the range of microwave-radiation

directed transfer increases with decrease in wavelength and reaches several kilometers for submillimeter waves.

* * *

This work was performed under the support of Advanced Energy Technologies Ltd. and also the Russian Foundation for Basic Research, Project No 09-07-13593-ofi-ts.

REFERENCES

[1] Braun A., Korn G., Liu X. *et al.*, *Opt. Lett.*, **20** (1995) 73.
[2] Nibbering E. T. J., Curley P. F., Grillon G. *et al.*, *Opt. Lett.*, **21** (1996) 62.
[3] Brodeur A., Chien C. Y., Ilkov F. A. *et al.*, *Opt. Lett.*, **22** (1997) 304.
[4] Dormidondov A. E., Valuev V. V., Dmitriev V. L. *et al.*, *Proc. SPIE*, **6733** (2007) 67332S.
[5] Chateauneuf M., Payeur S., Dubois J. and Kieffer J.-C., *Appl. Phys. Lett.*, **92** (2008) 091104.
[6] Zvorykin V. D., Levchenko A. O., Ustinovsky N. N. and Smetanin I. V., *JETP Lett.*, **91** (2010) 226.
[7] Smetanin I. V., Zvorykin V. D., Levchenko A. O. and Ustinovsky N. N., *J. Russ. Laser Res.*, **31** (2010) 495.
[8] Askarjan G. A., *Sov. Phys. JETP*, **28** (1969) 732.
[9] Vainshtein L. A., *Electromagnetic Waves* (Radio i Svyaz, Moscow) 1988 (in Russian).
[10] Cros B., Courtois C., Matthieussent G. *et al.*, *Phys. Rev. E*, **65** (2002) 026405.
[11] Dorchies F., Marques J. R., Cros B. *et al.*, *Phys. Rev. Lett.*, **82** (1999) 4655.
[12] Jackel S., Burris R., Grun J. *et al.*, *Opt. Lett.*, **20** (1995) 1086.
[13] Borghesi M., Mackinnon A. J., Gaillard R. *et al.*, *Phys. Rev. E*, **57** (1998) R4899.
[14] Basov N. G., Vadkovsky A. D., Zvorykin V. D. *et al.*, *Quantum Electron.*, **24** (1994) 13.
[15] Zvorykin V. D., Levchenko A. O., Molchanov A. G. *et al.*, *Bull. Lebedev Phys. Inst.*, **37** (2010) N2, 60.
[16] Raiser Yu. P., *Gas Discharge Physics* (Nauka, Moscow) 1987 (in Russian) (English translation: (Springer, Berlin) 1991).
[17] Engelhardt A. G., Phelps A. V. and Risk C. G., *Phys. Rev. A*, **135** (1964) 1556.
[18] Gordeyev O. A., Kalinin A. P., Komov A. L. *et al.*, in *Reviews on the Thermophysical Properties of Substances*, Vol. **5**, no. 55 (Institute of High Temperatures of the Russian Academy of Sciences, Moscow) 1985 (in Russian).
[19] Stratton J. A., *Electromagnetic Theory* (McGraw-Hill, London) 1941.